Electrosynthesis of Green Urea by co-reduction of N_2 and CO_2 Using Dual Active Sites of Copper Phthalocyanine Nanotube

Jit Mukherjee[1], Sourav Paul[1], Ashadul Adalder[1], Samadhan Kapse[2], Ranjit Thapa[2], Sumit Mandal[3], Biswajit Ghorai[1], Sougata Sarkar[1] and Uttam Kumar Ghorai[1]*

[1]Department of Industrial Chemistry & Applied Chemistry, Swami Vivekananda Research Centre, Ramakrishna Mission Vidyamandira, Belur Math, Howrah, 711202, India
[2]Department of Physics, SRM University – AP, Amaravati, Andhra Pradesh, 522240, India
[3]Department of Physics, Vidyasagar college, Kolkata -700006, India

Corresponding author:
*Email: uttam.indchem@vidyamandira.ac.in; uttamindchem00@gmail.com

Abstract: Green synthesis of urea under ambient conditions by electrochemical co-reduction of N_2 and CO_2 gases using effective electrocatalyst essentially pushes the conventional two steps ($N_2 + H_2 = NH_3$ & $NH_3 + CO_2 = CO(NH_2)_2$) industrial process at high temperature and high pressure, to the brink. The single step electrochemical green urea synthesis process has hit a roadblock due to the lack of efficient and economically viable electrocatalyst with multiple active sites for dual reduction of N_2 and CO_2 gas molecules to urea. Herein, copper phthalocyanine nanotubes (CuPc NTs) having multiple active sites (such as metal center, Pyrrolic-N3, Pyrrolic-N2, and Pyridinic-N1) are reported to exhibit urea yield of 143.47 $\mu g\ h^{-1}\ mg^{-1}_{cat}$ and FE of 12.99% at –0.6 V vs RHE by co-reduction of N_2 and CO_2. Theoretical calculation suggests that Pyridinic-N1 and Cu centers are responsible to form C-N bonds for urea by reduction of N_2 to NN* and CO_2 to *CO respectively. This study not only provides the new mechanistic insight about the successful electro-reduction of dual gases (N_2 and CO_2) in a single component, but also helps to select for rational design of the efficient noble metal-free electrocatalyst for the synthesis of green urea.

KEYWORDS: copper phthalocyanine, urea, electrochemical co-reduction, green synthesis, dual active sites

Introduction:

With the global annual production of 100 million tons, urea is considered to be one of the important nitrogen sources for fertilizer industry [1-2]. Industrial urea is synthesized by the following two consecutive steps. First, the reaction of nitrogen and hydrogen ($N_2 + H_2 \rightarrow NH_3$) by the Haber-Bosch process at high temperature and pressure (350–550°C, 150–350 bar); followed by the reaction of NH_3 and CO_2 [$NH_3 + CO_2 \rightarrow CO(NH_2)_2$] under mild reaction conditions (170–200°C and 200–250 bar) [3-4]. The sequential reactions are carried out for several cycles to increase the conversion efficiency [2]. For the first step, fixation of N_2 and H_2 is an energy as well as capital intensive process due to difficulty in cleaving the N≡N bond. Extensive research works have been reported on electrochemical N_2 fixation to NH_3 in water medium under ambient conditions [5-13]. In this electrochemical method, isolation of NH_3 gas with high purity from electrolyte solution is troublesome. In the second step, CO_2 fixation on the substrate and its separation is one of the major challenging tasks for the further reaction with NH_3 to end up in urea. Overall, the two step process for large scale production of urea, consumes high energy and this industrial process is not at all cost effective. On the other hand, electrochemical urea synthesis by the co-reduction of N_2 and CO_2 ($N_2 + CO_2 + 6H^+ + 6e^- \rightarrow CO\ (NH_2)_2 + H_2O$) using efficient electrocatalyst in water medium under ambient conditions would be an alternative way in the upcoming days. Chen et al. [14] developed a noble metal based PdCu alloy nanoparticles on TiO_2 nanosheets for electrochemical urea preparation in water with formation rate of 3.36 mmol g^{-1} h^{-1} and FE of 8.92% at –0.4 V vs RHE. Non-noble metal Bi-$BiVO_4$ heterostructure was designed by Yuan et al. [15] for electrochemical urea synthesis by co-activation of N_2 and CO_2, and the Mott-Schottky catalyst showed the urea yield rate of 5.91 mmol h^{-1} g^{-1} at –0.4 V vs RHE along with FE of 12.55%. Recently, their research group have also fabricated $BiFeO_3/BiVO_4$ based heterojunction showing urea yield rate of 4.94 mmol h^{-1} g^{-1} with FE of 17.18% at –0.4 V vs

RHE in 0.1 M $KHCO_3$ [16]. All the strategies using heterostructure and alloys for urea synthesis forming C-N bond by the co-reduction of N_2 and CO_2, have not been reached the bench mark in term of urea yield rate and FE for practical applications. To achieve the high urea yield and FE, the following factors are to be taken into account. First, as catalysis being a surface phenomenon, higher specific surface area with easier adsorption of the gases (N_2 and CO_2) and facile desorption of the product (urea) is an absolute necessity. Secondly, catalyst must possess multiple active sites for co-reduction of gaseous molecules (N_2 and CO_2) in the similar potential range. Thirdly, electrocatalyst must have specificity and selectivity towards simultaneous reduction of N_2 sources (N_2, nitrate, nitrite, NO etc.) and CO_2 by the formation of C-N bond coupling [14, 17-19]. And finally, the suppression of hydrogen evolution reaction (HER), choice of electrolyte and catalyst are very crucial for electrochemical urea synthesis [14]. In this regard, electrocatalyst having multiple active sites and selectivity towards both NRR and CO_2RR under the similar potential window may be effective for urea synthesis in water medium at standard temperature and pressure (STP). Karapinar et al. [20] developed CuPc-CNT electrocatalyst which showed the electroreduction of CO_2 into CO with large FE at low overpotential. Prof. Hu and coworkers [21] studied that iron phthalocyanine/carbon (FePc/C) is an effective NRR electrocatalyst which showed the yield rate of NH_3 to be 10.25 μg h^{-1} mg_{cat}^{-1} at low potential of –0.3 V and FE of 10.50%. Recently, we have reported transition metal phthalocyanine nanostructures having multiple active sites (metal center, Pyrrolic-N3, Pyrrolic-N2, and Pyridinic-N1) as an efficient NRR electrocatalyst [22-23]. Therefore, metal phthalocyanine as an electrocatalyst have shown the potential as an effective activator to co-reduce N_2 and CO_2 due to their multiple active sites under ambient conditions which is yet to be excavated by the research community.

In this article, we have demonstrated CuPc nanotubes, synthesized through solvothermal method, as an efficient catalyst for the electrosynthesis of green urea. As prepared CuPc nanotubes deliver the urea yield rate of 143.47 μg h^{-1} mg^{-1}_{cat} and FE of 12.99% at –0.6 V vs RHE under ambient conditions. DFT calculation helps to identify the various active sites of CuPc molecules responsible for the formation of C–N bond via coupling of N_2 and CO_2.

Results and discussion: Prior to the synthesis of catalyst, theoretical calculations are performed to understand the reaction mechanism and to identify the catalytic sites in copper phthalocyanine (CuPc) favoring urea synthesis by coupling N_2 and CO_2. In this context, the urea synthesis is a complex reaction with the following major challenges; (i) N_2 adsorption, (ii) CO_2 adsorption and conversion to CO, and (iii) competing HER and ammonia (NH_3) formation. Recently, the phthalocyanine systems are reported as an efficient electrocatalyst for N_2 fixation due to unsaturated configuration of active sites [21-22]. Therefore, we considered five different types of possible active sites (Cu, C, N1, N2, N3) in the CuPc model that are highlighted with different colors in **Figure 1b**. Firstly, we estimated the N_2 adsorption energy on active sites of CuPc as shown in **Figure 1c**. It is seen that the N_2 adsorption free energies (*NN) of all sites are exothermic in nature and obtained in the following order: Pyridinic-N1 (–0.108eV) > Pyrrolic-N2 (–0.088eV) > Pyrrolic-N3 (–0.083eV) > Carbon (–0.055eV) > Cu (–0.038eV). Importantly, the Pyridinic-N1 is found to be the preferred site for N_2 adsorption (end on configuration). The urea synthesis process also depends on the evolution of CO through CO_2 reduction, which is highly influenced by the adsorption of COOH intermediate on the active site [24]. It is well known that the Cu-based catalysts are ideal to catalyze CO_2 into useful products [20, 25-26]. Therefore, we considered Cu center of CuPc NTs to reduce CO_2 into CO. We observed that the adsorption free energy of COOH (*COOH) is 0.39 eV on Cu active site of CuPc, which is decreased to 0.31 eV in presence of adsorbed N_2 on Pyridinic site (**Figure 1d**). The charge transfer seems to occur on Cu site and investigated through bader charge analysis. The bader charge of Cu center is –0.23e and +1.12e in pristine CuPc and N_2 adsorbed CuPc respectively. Thus, the gain of charge on Cu center due to neighboring adsorbed N_2 is the reason for lowering of free energy for *COOH (*NN), which improves the ease of CO_2 electroreduction.

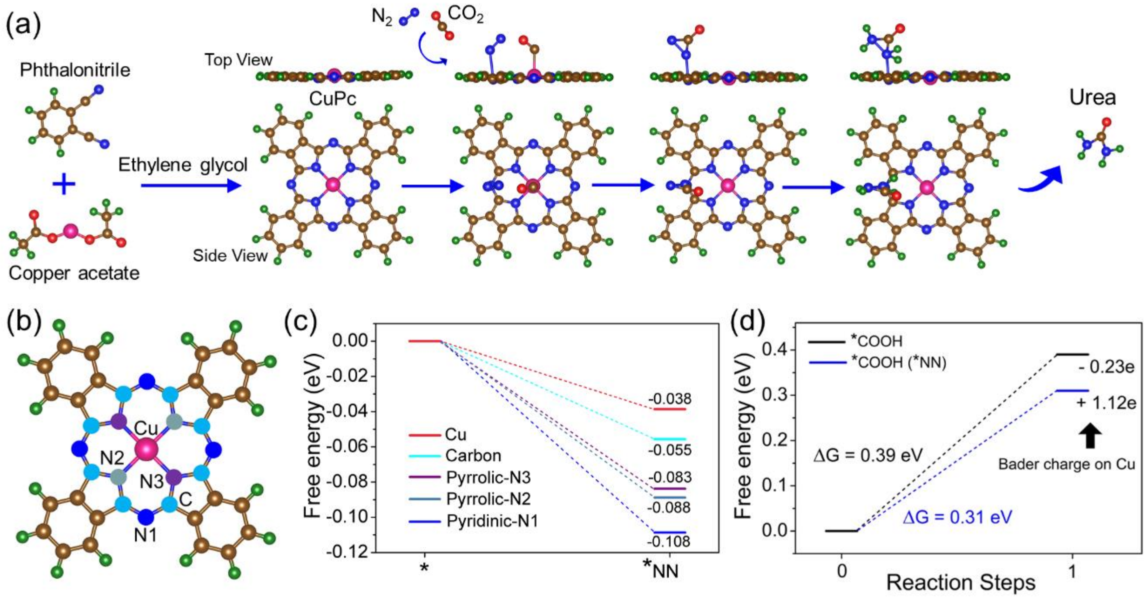

Figure 1: *(a) Demonstrate the schematic representation of copper phthalocyanine synthesis and co-reduction of nitrogen and carbon dioxide to produce urea; (b) Represents the model of CuPc and possible active sites denoted with different colors. (c) Demonstrates the free energy profile of* N_2 *adsorption on the active sites of CuPc (d) Represents COOH adsorption on Cu center of CuPc with and without neighbouring* N_2 *molecule. Dotted lines are guide to the eye.*

The CuPc NTs were synthesised by ethylene glycol assisted solvothermal technique in our earlier report [27] [**Figure 1a** & see the SI for details]. The role of ethylene glycol for the synthesis of metal phthalocyanine is explained in our previous work [22]. The detailed reaction mechanism for the formation of CuPc molecule is shown in the **Figure S1**. The phase purity identification and crystalline structure of chemically synthesized CuPc nanotubes are examined by XRD technique, as shown in **Figure 2a**. The peaks at 6.9° and 9.1° in the pattern specify the formation of pure β phase. All the peaks, indexed as $(\bar{1}01)$, (101), (002), (200), $(\bar{2}02)$, $(\bar{1}03)$, $(\bar{3}01)$ and (103) in the XRD pattern are well matched with standard JCPDS card (No. 39-1881).

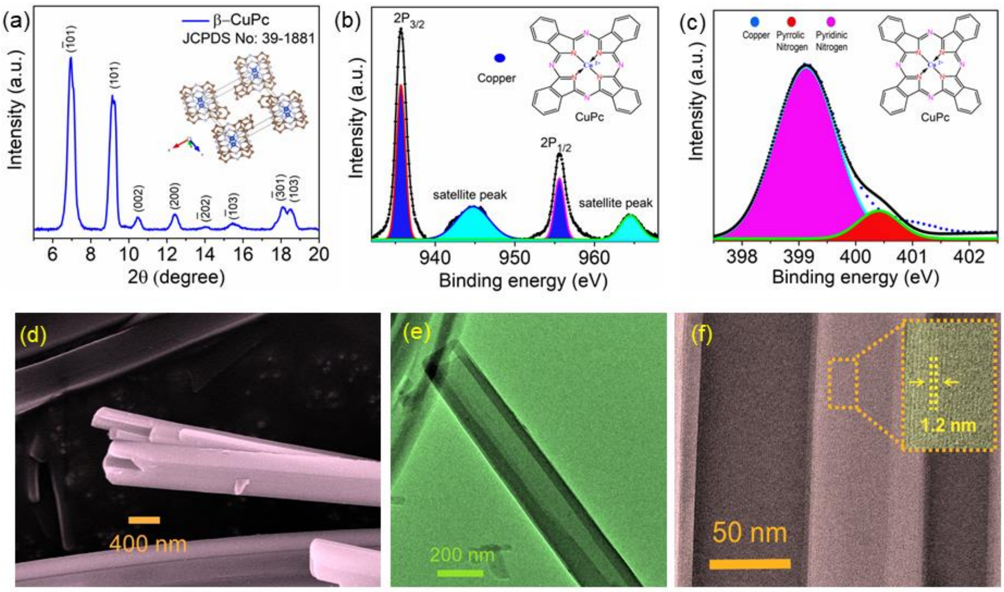

Figure 2: *(a) X-ray diffraction pattern of CuPc nanotubes; (b) & (c) High resolution XPS spectra of the Cu 2p doublet and N 1s respectively; (d) FESEM image of CuPc nanotubes having wall thickness in the range of 70-120 nm; (e) TEM image of a hollow nanotube; (f) HRTEM lattice image of CuPc nanotubes.*

Various chemical bonds present in the CuPc nanotubes are confirmed by FTIR spectra which are shown in the **Figure S2**. The most significant peak at 1166 cm^{-1} is ascribed to the existence of Cu–N bonding in the CuPc molecule [28]. The peaks at 901, 1068, 1090, and 1119 cm^{-1} are assigned to pyrrole in plane modes of CuPc and the peak at 879 cm^{-1} indicates the pyrrole out-of-plane modes of phthalocyanine. The peak at 1288 and 1334 cm^{-1} can be assigned to C=N–C bridge sites in CuPc [28, 29]. **Figure S3** shows the survey scan spectrum which confirms the coexistence of major constituent's elements Cu, N and C in the CuPc molecule. In **Figure 2b**, the peaks at 935.64 eV and 955.63 eV are assigned to the electronic states of Cu $2p_{3/2}$ and Cu $2p_{1/2}$ respectively [28]. The satellite peak indicates the divalent nature of Cu in the CuPc molecule [28]. A high resolution spectrum of N1s is presented in the **Figure 2c,** which consists of two peaks at 399.13 eV and 400.39 eV indicating the pyridinic nitrogen and pyrrolic nitrogen group respectively in the CuPc molecule [28]. The FESEM image of the chemically synthesized CuPc nanotubes is shown in **Figure 2d.** The length and diameter of the 1D CuPc nanotubes are found to be around 4 μm and 220–400 nm respectively. **Figure 2e** shows the TEM (transmission electron microscopy) image of the CuPc hollow nanotube having wall thickness less than ~100 nm. The high resolution microscopic (HRTEM) image is shown in the **Figure 2f** and the lattice spacing of the CuPc nanotubes is 1.2 nm which is related to the $(\bar{1}01)$ plane.

To study the electrocatalytic activity of CuPc NTs, electrochemical measurements were performed in a (N_2 + CO_2) purged and Ar saturated 0.1 M $KHCO_3$ electrolyte using H-type cell at room temperature and normal pressure (Shown in **Figure S4**). **Figure S5** shows the linear sweep voltammetry (LSV) curve of CuPc NTs recorded at 50 mVs^{-1} where LSV curve shows the enhanced current densities in the potential range of –0.3 to –0.8 V (vs RHE) in comparison to that of the Ar saturated solution, indicating the feasibility of co-reduction for electrocatalytic urea synthesis [14-15]. The quantitative determination of urea yield by co-reduction of dual gas (N_2 and CO_2) is accomplished using CuPc NTs, and time dependent chronoamperometry measurements were carried out at different applied potentials in dual gas (N_2 + CO_2) saturated electrolyte (shown in **Figure 3a**). The UV–vis absorption spectrum of electrolyte with distinctive absorption of 525 nm at various potential ranges is presented in **Figure 3b** and the maximum was found at –0.6 V vs RHE. The produced urea was estimated by diacetyl-monoxime method at different potentials (see the detailed procedure in SI). The related calibration curve for the estimation of urea is shown in the **Figure S6**. The urea yield and corresponding FE of the produced urea in a potential window is depicted in the **Figure 3c.** The CuPc NTs deliver maximum urea yield rate and FE are of 143.47 μg h^{-1} mg^{-1}_{cat} at –0.6 V vs RHE and 14.83 % at –0.3 V vs RHE respectively. The high urea yield rate is attributed to the C-N bond formation through co-reduction of N_2 and CO_2 in the CuPc molecule by the Pyridinic N sites and Cu metal centre respectively, which is further verified by our DFT calculation. Additionally, it is observed that urea yield rate increases with negative potentials until –0.6 V vs RHE and the rate decreases due to the competitive reaction between H_2 and N_2 in the electrode surface. Stability and recyclability are the important parameters to verify the efficacy of the catalyst performance for real life applications. CuPc NTs electrocatalyst has negligible changes in urea yield rate and FE during recycling experiment for five consecutive cycles (**Figure 3d**). **Figure S7** shows the long term electrolysis for 10 h at –0.6 V vs RHE in 0.1 $KHCO_3$ which demonstrates the good catalytic stability of CuPc NTs. After 10 h electrolysis, the urea yield rate and corresponding FE of CuPc NTs slightly decreases from its initial value (135.89 μg h^{-1} mg^{-1}_{cat} and 10.04%). In order to check the stability of the catalyst after rigorous electrolysis (10 h), we have examined the catalyst through XRD and the consistency remains intact with that one prior to catalysis (**Figure S8**).

All the results clearly indicate the durable and stable character of CuPc NTs electrocatalyst under ambient conditions for electrochemical urea synthesis through co-reduction of N_2 and CO_2. To further verify that, urea is produced through co-reduction method, the controlled electrolysis has been carried out in dual gas (N_2 + CO_2), Ar saturated solution, bare carbon paper substrate and under an open circuit potential at –0.6 V vs RHE for 2 h. Negligible amount of urea was detected for all the cases as shown in the **Figure S9**, suggesting that CuPc NTs is highly active candidate for green urea synthesis.

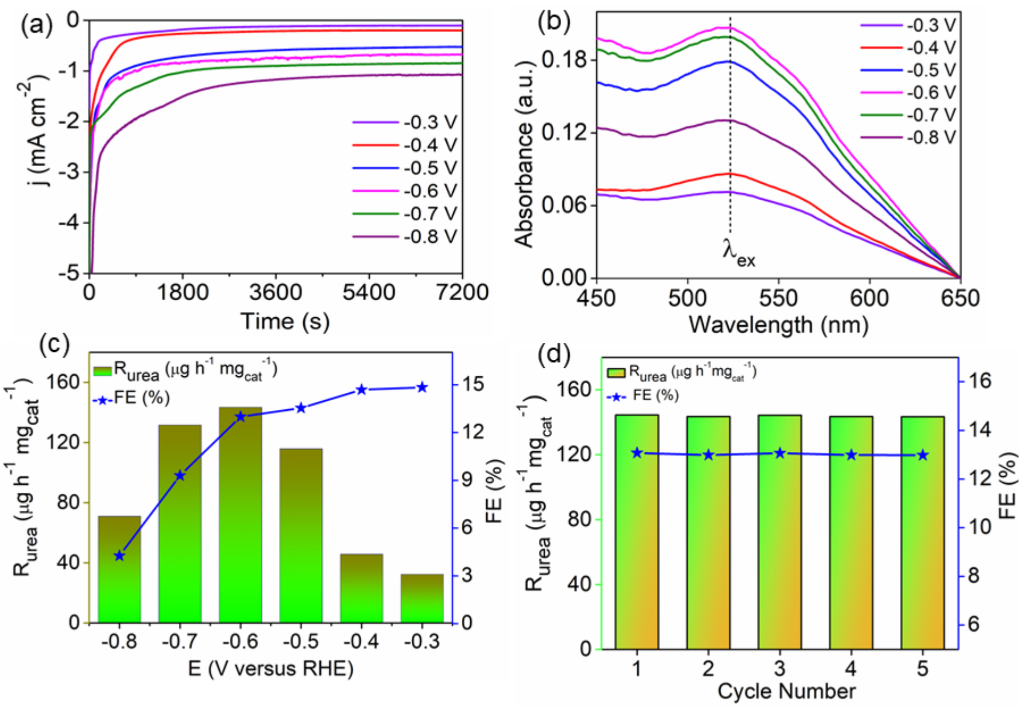

Figure 3: *(a) Time reliant current density (j) curves for CuPc NTs at various potential; (b) UV-vis absorption spectra of the electrolytes; (c) Urea yield rate and FE with* N_2 *and* CO_2 *as feeding gas at different potentials for CuPc NTs; (d) The urea yield rate and FE of CuPc nanotubes at –0.6 V vs RHE during recycling tests for five times.*

Further, we proposed the entire reaction mechanism of urea synthesis on CuPc via the dual active sites, namely Pyridinic-N1 and Cu site for N_2 and CO_2 co-reduction respectively. To understand the process of urea synthesis, see the schematic diagram in **Figure 4**.

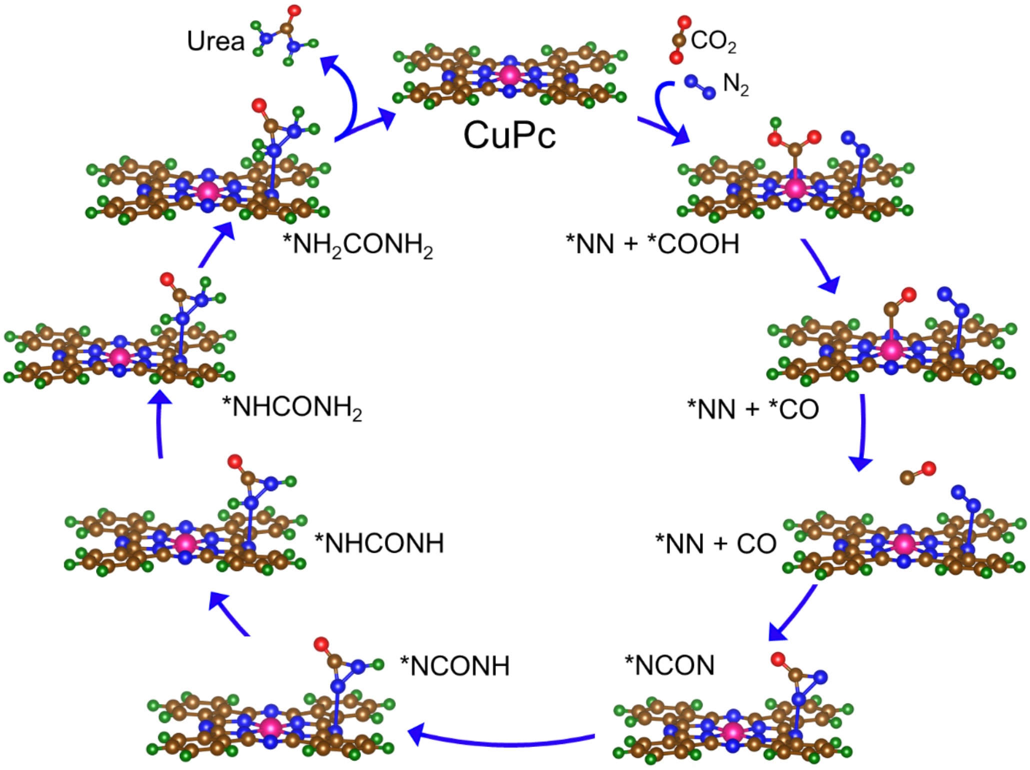

Figure 4 *Demonstrating the various steps of urea synthesis during co-reduction of N_2 and CO_2 on CuPc. (the symbol * denoted for the adsorption) The Cu, N, O, C, H atoms are denoted with pink, blue, red, wine, and green color sphere respectively. For easy understanding of reaction mechanism, the free H atom not shown in figure during hydrogenation of *NCON group.*

The full free energy profile of urea synthesis is demonstrated in **Figure 5a**. The first step includes the adsorption of N_2 on Pyridinic-N1 site and CO_2 on Cu site of CuPc. Free CO molecule from Cu site is released during CO_2 reduction to help in the formation of *NCON intermediate by making the bond with neighboring adsorbed N_2 molecule. The distance between N-N of N_2 molecule is 1.12 Å, which is increased to 1.37 Å after the CO attachment indicating the weakening of the triple bond of nitrogen molecule. Here, the reaction step *N_2 + CO (3^{rd}) to *NCON (4^{th}) is found to be the potential determining step and the corresponding overpotential is 1.72 V. Later, the hydrogenation of *NCON group takes place towards the synthesis of NH_2CONH_2 (urea). It is observed that the free energy of *NNH (1.88 eV) has higher positive value than that of *NCON (1.57 eV) that indicates less possibility of the NH_3 formation. Therefore, the energy of NCON intermediate is an important parameter to specify the possibility of production of urea on CuPc NTs. In **Figure 5b**, we show that the free energy of hydrogen (ΔG_{H*}) on Cu is +2.01 eV, much higher than *COOH, which improves the faradic efficiency of urea synthesis by greatly suppressing HER. Also, the higher values of ΔG_{H*} on Pyrrolic-N_2 (+0.95 eV), Pyrrolic-N_3 (+1.07 eV) and Carbon (+1.43 eV) indicate low HER performance of the present catalyst. Whereas, the hydrogen adsorption does not occur on Pyridinic-N1 site of CuPc. Especially, high positive value of ΔG_{H*} limits the H poisoning on the CuPc surface. Further, we performed the charge density difference study to visualize electron transfer behavior during the adsorption of COOH on Cu site (**Figure 5c,d**). The electrons accumulation (yellow color isosurface) is observed on the bond between the COOH and Cu center that confirms the adsorption of COOH. The estimated bader charge of Cu in pristine CuPc (–0.23e) is reduced to –0.41e in *COOH which signifies the transfer of charge (0.18e) from Cu to COOH during the adsorption. Overall, we propose the reaction mechanism of urea synthesis using co-reduction of N_2 and CO_2 on CuPc NTs with insignificant probability of NH_3 formation. Also, we demonstrate that the possibility of HER is negligible and positive hydrogen free energy ensures the implausibility of hydrogen poisoning on CuPc.

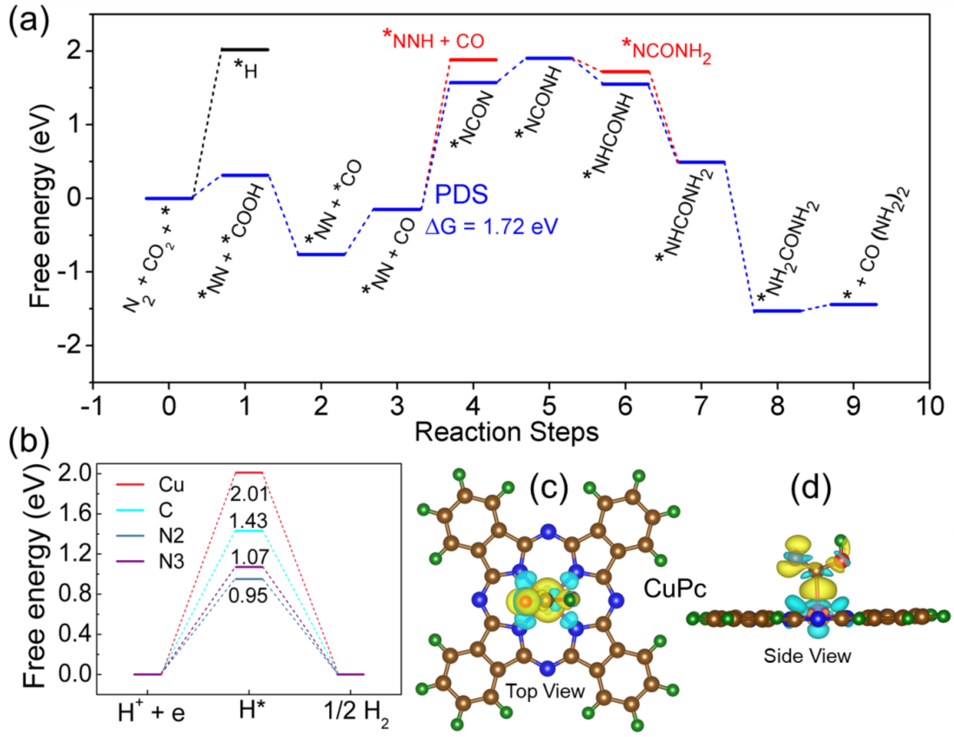

Figure 5: *(a) Demonstrates the full free energy profile of urea synthesis and hydrogen adsorption on Cu center (b) Represents the free energy diagram of hydrogen evolution reaction on active sites of CuPc. The Charge density difference analysis of COOH adsorption on Cu center of CuPc is shown in (c) Top view (d) Side view. The charge accumulation and depletion are represented by the yellow and cyan color region respectively (Isosurface value = 0.001). Dotted lines are guide to the eye.*

Conclusion: In summary, β-CuPc NTs has been proposed as an efficient electrocatalyst for co-reduction of mixed gas ($N_2 + CO_2$) to synthesize urea under ambient conditions. The CuPc NTs deliver a high FE 14.83 % at –0.3 V vs RHE and urea yield rate of 143.47 $\mu g\ h^{-1}\ mg^{-1}_{cat}$ at potential of –0.6 V vs RHE in 0.1 M $KHCO_3$ with good durability and long term stability. DFT calculation predicts that Pyridinic-N1 in CuPc is responsible for N_2 reduction and metal centre plays an important role for CO_2 reduction. Moreover, the possible co-reduction mechanism for urea synthesis is presented. This study not only provides us the co-reduction of N_2 and CO_2 gases using cost effective CuPc NTs catalyst with multiple actives sites for urea synthesis, but also opens up a new pathway to the rational design of other transitional metal based electrocatalysts having multiple active sites for N_2 and CO_2 gas fixation applications.

Author information

FAX: 2654-1123; Phone: 91 33 26549181

ORCID

Uttam Kumar Ghorai: 0000-0003-0537-598X

Sourav Paul: 0000-0002-6215-8183

ACKNOWLEDGEMENTS: The authors acknowledge Mr. S. Guchait (IACS) for TEM measurement. The authors also acknowledge Prof. K. K. Chattopadhyay (JU) for FESEM facility. The authors thank High Performance Computing Center, SRM IST for providing the computational facility. UKG acknowledges the Teachers Associateship for Research Excellence (TARE) scheme (TAR/2018/000763) of SERB, Govt. of India for research grant and fellowship. UKG acknowledges the central DST-FIST programme (SR/FST/College-287/2015) for providing financial support. UKG thanks to DBT star college scheme (BT/HRD/11/036/2019) for funding. UKG also acknowledges Science & Technology and Biotechnology Department, Govt. of West Bengal for providing the financial support [199 (Sanc.)/ST/P/S&T/6G-12/2018]. R.T. thanks Board of Research in Nuclear Sciences (BRNS), India, for the financial support (Grant Nos. 37(2)/20/14/2018-BRNS/37144). AA wishes to thank Science & Technology and Biotechnology Department, Govt. of West Bengal for providing the financial support (ST/P/S&T/6G-6/2019).

AUTHOR CONTRIBUTIONS: UKG conceived the idea and designed the experiments. JM, BG, AA and SS synthesized the catalyst and performed the XRD, FTIR, UV-vis. SP, JM, AA and SM carried out all the electrochemical measurements and analyzed the results. SK and RT performed the theoretical (DFT) calculations. RT, SK, JM and SP analyzed the DFT results. All authors contributed to write the manuscript. UKG supervised the entire project.

COMPETING INTERESTS: UKG, JM, SP and AA have filed an Indian Patent application (202131027290) regarding the electrochemical synthesis of green urea process under ambient conditions.

References:

(1) Erisman, J. W.; Sutton, M. A.; Galloway, J.; Klimont, Z.; Winiwarter, W. How a Century of Ammonia Synthesis Changed the World. *Nat. Geosci.* **2008**, *1* (10), 636–639.

(2) Barzagli, F.; Mani, F.; Peruzzini, M. From Greenhouse Gas to Feedstock: Formation of Ammonium Carbamate from CO_2 and NH_3 in Organic Solvents and Its Catalytic Conversion into Urea under Mild Conditions. *Green Chem.* **2011**, *13* (5), 1267–1274.

(3) Meessen, J. Urea Synthesis. *Chemie-Ingenieur-Technik* **2014**, *86* (12), 2180–2189.

(4) Krase, N. W.; Gaddy, V. L. Synthesis of Urea from Ammonia and Carbon Dioxide. *Ind. Eng. Chem.* **1922**, *14* (7), 611–615.

(5) Yuan, M.; Li, Q.; Zhang, J.; Wu, J.; Zhao, T.; Liu, Z.; Zhou, L.; He, H.; Li, B.; Zhang, G. Engineering Surface Atomic Architecture of NiTe Nanocrystals Toward Efficient Electrochemical N_2 Fixation. *Adv. Funct. Mater.* **2020**, *30* (39), 1–9.

(6) Zhang, J.; Ji, Y.; Wang, P.; Shao, Q.; Li, Y.; Huang, X. Adsorbing and Activating N_2 on Heterogeneous Au–Fe_3O_4 Nanoparticles for N_2 Fixation. *Adv. Funct. Mater.* **2020**, *30* (4), 1–8.

(7) Yuan, M.; Zhang, H.; Gao, D.; He, H.; Sun, Y.; Lu, P.; Dipazir, S.; Li, Q.; Zhou, L.;

Li, S.; Liu, Z.; Yang, J.; Xie, Y.; Zhao, H.; Zhang, G. Support Effect Boosting the Electrocatalytic N_2 Reduction Activity of Ni_2P/N, P-Codoped Carbon Nanosheet Hybrids. *J. Mater. Chem. A* **2020**, *8* (5), 2691–2700.

(8) Wang, J.; Huang, B.; Ji, Y.; Sun, M.; Wu, T.; Yin, R.; Zhu, X.; Li, Y.; Shao, Q.; Huang, X. A General Strategy to Glassy M-Te (M = Ru, Rh, Ir) Porous Nanorods for Efficient Electrochemical N_2 Fixation. *Adv. Mater.* **2020**, *32* (11), 1–9.

(9) Yang, C.; Huang, B.; Bai, S.; Feng, Y.; Shao, Q.; Huang, X. A Generalized Surface Chalcogenation Strategy for Boosting the Electrochemical N_2 Fixation of Metal Nanocrystals. *Adv. Mater.* **2020**, *32* (24), 1–10.

(10) Zheng, J.; Lyu, Y.; Qiao, M.; Veder, J. P.; Marco, R. D.; Bradley, J.; Wang, R.; Li, Y.; Huang, A.; Jiang, S. P.; Wang, S. Tuning the Electron Localization of Gold Enables the Control of Nitrogen-to-Ammonia Fixation. *Angew. Chemie - Int. Ed.* **2019**, *58* (51), 18604–18609.

(11) Wu, B.; Lin, Y.; Wang, X.; Chen, L. Recent Advances on Electrocatalytic Fixation of Nitrogen under Ambient Conditions. *Mater. Chem. Front.* **2021**. https://doi.org/10.1039/d1qm00269d.

(12) Yan, D.; Li, H.; Chen, C.; Zou, Y.; Wang, S. Defect Engineering Strategies for Nitrogen Reduction Reactions under Ambient Conditions. *Small Methods* **2019**, *3* (6), 1–21.

(13) Wei, Z.; Zhang, Y.; Wang, S.; Wang, C.; Ma, J. Fe-Doped Phosphorene for the Nitrogen Reduction Reaction. *J. Mater. Chem. A* **2018**, *6* (28), 13790–13796.

(14) Chen, C.; Zhu, X.; Wen, X.; Zhou, Y.; Zhou, L.; Li, H.; Tao, L.; Li, Q.; Du, S.; Liu, T.; Yan, D.; Xie, C.; Zou, Y.; Wang, Y.; Chen, R.; Huo, J.; Li, Y.; Cheng, J.; Su, H.; Zhao, X.; Cheng, W.; Liu, Q.; Lin, H.; Luo, J.; Chen, J.; Dong, M.; Cheng, K.; Li, C.; Wang, S. Coupling N_2 and CO_2 in H_2O to Synthesize Urea under Ambient Conditions. *Nat. Chem.* **2020**, *12* (8), 717–724.

(15) Yuan, M.; Chen, J.; Bai, Y.; Liu, Z.; Zhang, J.; Zhao, T.; Wang, Q.; Li, S.; He, H.; Zhang, G. Unveiling Electrochemical Urea Synthesis by Co-Activation of CO_2 and N_2 with Mott–Schottky Heterostructure Catalysts . *Angew. Chemie* **2021**, *133* (19), 11005–11013.

(16) Yuan, M.; Chen, J.; Bai, Y.; Liu, Z.; Zhang, J.; Zhao, T.; Shi, Q.; Li, S.; Wang, X.; Zhang, G. Electrochemical C-N Coupling with Perovskite Hybrids toward Efficient Urea Synthesis. *Chem. Sci.* **2021**, *12* (17), 6048–6058.

(17) Feng, Y.; Yang, H.; Zhang, Y.; Huang, X.; Li, L.; Cheng, T.; Shao, Q. Te-Doped Pd Nanocrystal for Electrochemical Urea Production by Efficiently Coupling Carbon Dioxide Reduction with Nitrite Reduction. *Nano Lett.* **2020**, *20* (11), 8282–8289.

(18) Meng, N.; Huang, Y.; Liu, Y.; Yu, Y.; Zhang, B. Electrosynthesis of Urea from Nitrite and CO_2 over Oxygen Vacancy-Rich ZnO Porous Nanosheets. *Cell Reports Phys. Sci.* **2021**, *2* (3), 100378.

(19) Shibata, M.; Furuya, N. Simultaneous Reduction of Carbon Dioxide and Nitrate Ions at Gas-Diffusion Electrodes with Various Metallophthalocyanine Catalysts. *Electrochim. Acta* **2003**, *48* (25–26), 3953–3958.

(20) Karapinar, D.; Zitolo, A.; Huan, T. N.; Zanna, S.; Taverna, D.; Galvão Tizei, L. H.; Giaume, D.; Marcus, P.; Mougel, V.; Fontecave, M. Carbon-Nanotube-Supported Copper Polyphthalocyanine for Efficient and Selective Electrocatalytic CO_2 Reduction to CO. *ChemSusChem* **2020**, *13* (1), 173–179.

(21) He, C.; Wu, Z. Y.; Zhao, L.; Ming, M.; Zhang, Y.; Yi, Y.; Hu, J. S. Identification of FeN_4 as an Efficient Active Site for Electrochemical N_2 Reduction. *ACS Catal.* **2019**, *9* (8), 7311–7317.

(22) Ghorai, U.; Paul, S.; Ghorai, B.; Adalder, A.; Kapse, S.; Thapa, R.; Nagendra, A.; Gain, A. Scalable Production of Cobalt Phthalocyanine Nanotubes: Efficient and Robust Hollow Electrocatalyst for Ammonia Synthesis at Room Temperature. *ACS Nano* **2021**, *15* (3), 5230–5239.

(23) Murmu, S.; Paul, S.; Kapse, S.; Thapa, R.; Chattopadhyay, S.; N, A.; Jha, S. N.; B, D.; Ghorai, U. K. Unveiling the Genesis of the High Catalytic Activity in Nickel Phthalocyanine for Electrochemical Ammonia Synthesis. *J. Mater. Chem. A* **2021**. https://doi.org/10.1039/d1ta00766a.

(24) Singh, M. R.; Goodpaster, J. D.; Weber, A. Z.; Head-Gordon, M.; Bell, A. T. Mechanistic Insights into Electrochemical Reduction of CO_2 over Ag Using Density Functional Theory and Transport Models. *Proc. Natl. Acad. Sci. U. S. A.* **2017**, *114*

(42), E8812–E8821.

(25) Zhao, J.; Xue, S.; Barber, J.; Zhou, Y.; Meng, J.; Ke, X. An Overview of Cu-Based Heterogeneous Electrocatalysts for CO_2 Reduction. *J. Mater. Chem. A* **2020**, *8* (9), 4700–4734.

(26) Nitopi, S.; Bertheussen, E.; Scott, S. B.; Liu, X.; Engstfeld, A. K.; Horch, S.; Seger, B.; Stephens, I. E. L.; Chan, K.; Hahn, C.; Nørskov, J. K.; Jaramillo, T. F.; Chorkendorff, I. Progress and Perspectives of Electrochemical CO_2 Reduction on Copper in Aqueous Electrolyte. *Chem. Rev.* **2019**, *119* (12), 7610–7672.

(27) Das, B.; Samanta, M.; Sarkar, P.; Ghorai, U. K.; Mallik, A.; Chattopadhyay, K. K. Copper (II) Phthalocyanine (CuPc) Based Optoelectronic Memory Device with Multilevel Resistive Switching for Neuromorphic Application. *Adv. Electron. Mater.* **2021**, *7* (4), 1–11.

(28) Ghorai, U. K.; Das, S.; Saha, S.; Mazumder, N.; Sen, D.; Chattopadhyay, K. K. Efficient and Persistent Cold Cathode Emission from CuPc Nanotubes: A Joint Experimental and Simulation Investigation. *Dalt. Trans.* **2014**, *43* (24), 9260–9266.

(29) Jung, J. S.; Lee, J. W.; Kim, K.; Cho, M. Y.; Jo, S. G.; Joo, J. Rectangular Nanotubes of Copper Phthalocyanine: Application to a Single Nanotube Transistor. *Chem. Mater.* **2010**, *22* (7), 2219–2225.